A fast semi-analytic method for the computation of elastic edge singularities

Martin Costabel, Monique Dauge, Yvon Lafranche

Fast semi-analytic computation of elastic edge singularities

Martin COSTABEL, Monique DAUGE, Yvon LAFRANCHE

IRMAR, Campus de Beaulieu, Université de Rennes 1, 35042 Rennes Cedex, France

Abstract

The singularities that we consider are the characteristic non-smooth solutions of the equations of linear elasticity in piecewise homogeneous media near two dimensional corners or three dimensional edges. We describe here a method to compute their singularity exponents and the associated angular singular functions. We present the implementation of this method in a program whose input data are geometrical data, the elasticity coefficients of each material involved and the type of boundary conditions (Dirichlet, Neumann or mixed conditions). Our method is particularly useful with anisotropic materials and allows to "follow" the dependency of singularity exponents along a curved edge.

1. Introduction

In linear elasticity, problems are usually solved with industrial codes using the finite element method. However, when the elastic body has corners on its boundary, such as a polygon or a polyhedron, the solution obtained is inaccurate near the corners. The reason is that on such domains, elliptic boundary value problems admit singular solutions. Thus, special "tools" to acquire some knowledge about those solutions can be very useful.

We consider the linear equilibrium equations of an elastic material Ω, possibly heterogeneous : we suppose that Ω can be decomposed in several homogeneous parts Ω_k, with $k = 1, \ldots, K$. Here we treat corners in two dimensional domains and edges in three dimensional ones. The corners and edges in question are those of Ω, of course, but also those of any of the homogeneous subdomains Ω_k. The equations in Ω can be written in general form

$$L_k u = f \quad \text{in} \quad \Omega_k, \qquad k = 1, \ldots, K, \tag{1}$$

with boundary conditions on $\partial\Omega$ and transmission conditions at the interfaces between the Ω_k.

If Ω is two dimensional, from the general theory (see KONDRAT'EV [5], GRISVARD [4] or NICAISE [7]), we know that, near any of its corners $\mathcal{O}$, the solution can be seen as a sum of a regular part $u_{\rm reg}$ and a singular one $u_{\rm sing}$. Except in particular cases where logarithmic terms appear, $u_{\rm sing}$ can be expanded in the generalized form

$$u_{\rm sing} \sim \sum_{i=1}^{\infty} B_i \, r^{\nu_i} g_i(\theta) \tag{2}$$

where (r, θ) are the polar coordinates with $\mathcal{O}$ as origin, B_i the *stress intensity factors*, ν_i the *singularity exponents* (or eigenvalues) and $g_i(\theta)$ the *angular singular functions* (or eigenfunctions).

The numbers ν_i are real or complex and characterize, along with the associated angular functions g_i, the behaviour of the solution near $\mathcal{O}$. They only depend on the boundary conditions, on the geometry of the subdomains Ω_k, and on the material laws.

In the case of an edge, the description of the splitting into regular and singular parts is more complicated, see [3] for instance, but still involves singularity exponents ν_i and angular singular functions g_i, possibly changing along the edge.

We are interested here in the computation of those two quantities, taking into account expressions provided by the theoretical work [1]. The core of the method is the knowledge for each $\nu \in \mathbb{C}$ and each material index k, of an explicit solution basis of the homogeneous system without boundary conditions

$$L_k\big(r^\nu g(\theta)\big) = 0\,. \tag{3}$$

Applying the boundary and transmission conditions to these bases leads to the construction of a matrix $A(\nu)$ whose determinant is called "characteristic determinant". Singularity exponents are the roots of the equation $\det A(\nu) = 0$, whose solution is obtained using Cauchy integrals.

Such a method is known and has been put into practice for isotropic materials, see Nicaise & Sändig [8]. But up to now, the other methods proposed for anisotropic materials are more numerical and less analytic than ours.

By a finite element approach in the one dimensional domain Θ of the angular variable θ, Leguillon & Sanchez-Palencia in [6] construct a matrix whose eigenvalues are the singularity exponents. Yosibash in [11] and [12] uses a formulation of the problem based on a modified Steklov method and constructs also a matrix with a similar role, by the p-version of finite elements in a thin bi-dimensional annulus of the form $\{x \in \mathbb{R}^2;\ r_0 < r < r_1,\ \theta \in \Theta\}$.

The method of Papadakis & Babuška [10] is closer to ours : they solve numerically the equations (3) with transmission conditions and boundary conditions on *one* side by two initial value problems and construct a matrix $\widetilde{A}(\nu)$ with the boundary conditions on the other side and then find the roots of the characteristic determinant $\det \widetilde{A}(\nu)$ using Cauchy integrals.

The main advantage of our method is to remain as close as possible to the exact solution since the solution bases of the equation are known almost analytically (only the roots of a symbol associated with the system L_k have to be computed). In particular, the angular singular functions g_i belong to the spaces generated by the above mentioned bases. We stress again the fact that an important part of the calculation is made explicitly, which is essential considering accuracy and computation time.

In §2 and 3, we recall from [1] and [2] the determination of the solution bases of equations (3). In §4 the principles for the construction of the matrix $A(\nu)$ are explained and in §5 their numerical implementation is described. In section §6 and 7, we present the computation of the singularity exponents and of the angular singular functions. In §8 we treat some specific aspects of three dimensional geometries. Finally, to show the range of application of the method and compare with the earlier works, we give in §9 various examples in two and three dimensions, especially for anisotropic materials, and with different boundary conditions. We draw some conclusions in §10.

2. Theoretical aspects : the solution bases

In this section and in the following one, we concentrate upon the solution basis of equation (3) for one material. Thus we drop the material index k.

2.1 Definitions and notations

We denote by

- d the dimension of the space, $d = 2$ or 3,
- x_ℓ, $\ell = 1, \ldots, d$ the space variables in $\mathbb{R}^d$,
- Ω the domain,
- L the operator associated with the system of linear elasticity.

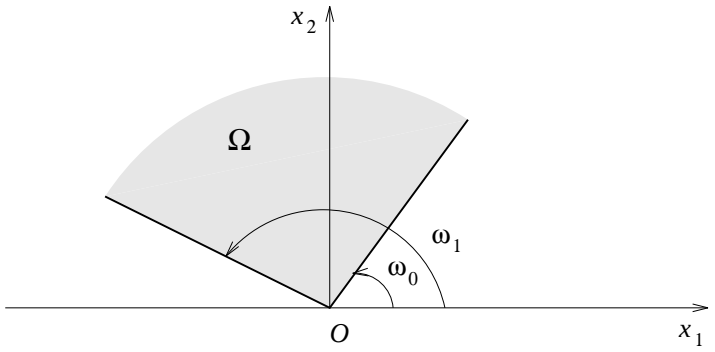

Figure 1

If $d = 2$, the domain Ω is polygonal : its boundary is the union of a finite number of segments whose ends are the *corners* of Ω. If $d = 3$, we consider domains with edges in the following sense : the boundary of Ω is the union of a finite number of smooth two dimensional surfaces whose boundaries are the edges of Ω. We assume that at each point $\mathcal{O}$ in an edge of Ω, the domain is locally diffeomorphic to a wedge (a plane sector times $\mathbb{R}$).

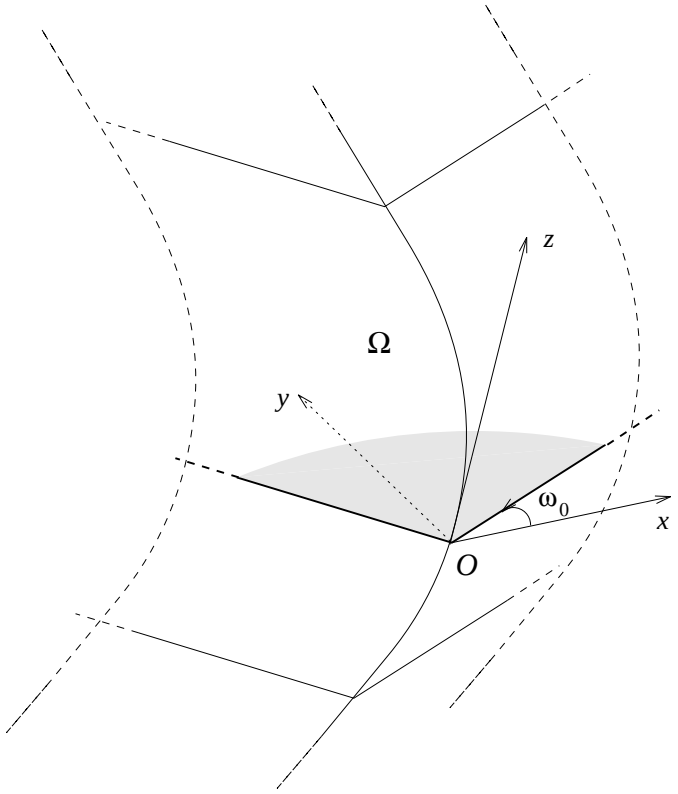

Figure 2

We consider the general elasticity equilibrium equation

$$Lu = f \quad \text{in} \quad \Omega.$$

The operator L is an elliptic $d \times d$ system of second order operators. Let $\mathcal{O}$ denote a corner of Ω in 2D and a point in an edge of Ω in 3D. We now have to define a reduced operator M associated with L at $\mathcal{O}$: the operator M acts in two variables and is the part of L which determines the singularities in $\mathcal{O}$.

In 2D, see Figure 1, $\mathcal{O}$ is a corner and $\omega = \omega_1 - \omega_0$ is the opening of the tangent sector to $\partial\Omega$ in $\mathcal{O}$. We denote by (r, θ) the polar coordinates with the origin taken in $\mathcal{O}$. In that case,

$$M \stackrel{\text{def}}{=} L.$$

In 3D, see Figure 2, $\mathcal{O}$ belongs to an edge of the domain. We introduce local axes $(\mathcal{O}; \vec{x}, \vec{y}, \vec{z})$ with $\mathcal{O}z$ tangent to the edge in $\mathcal{O}$. In the plane $(\mathcal{O}; \vec{x}, \vec{y})$, $\omega = \omega_1 - \omega_0$ is the opening of the tangent sector to $\partial\Omega$ in $\mathcal{O}$. We denote by (r, θ, z) the cylindrical coordinates with the origin taken in $\mathcal{O}$. The operator associated with the system $L(\partial x_1, \partial x_2, \partial x_3)$ is mapped in the local axes to the operator $\widetilde{L}_{\mathcal{O}}(\partial x, \partial y, \partial z)$. Singularity exponents depend on this operator, but without the tangent derivatives ∂z. Thus, in that case,

$$M(\partial x, \partial y) \stackrel{\text{def}}{=} \widetilde{L}_{\mathcal{O}}(\partial x, \partial y, 0).$$

2.2 The main result

M is then a $d \times d$ elliptic system in the plane variables (x, y). From Theorem 2.1 of [1], there holds :

> *The homogeneous problem (without boundary conditions)* $M\big(r^\nu \varphi(\nu, \theta)\big) = 0$ *has exactly* $2d$ *independent solutions* $\varphi_j(\nu, \theta), j = 1, \dots 2d$, *for any fixed* $\nu \in \mathbb{C}$.

The important point is that from [1], [2], we know an explicit formula for the solutions φ_j for any non integer ν. In order to describe it, let us introduce for $\alpha \in \mathbb{C}$ the Cayley transforms of the symbol M

$$M_+(\alpha) = M(\alpha + 1, i(\alpha - 1)) \quad \text{and} \quad M_-(\alpha) = M(1 + \alpha, i(1 - \alpha)).$$

As a consequence of ellipticity of the system, $\det M_+(\alpha)$ (resp. $\det M_-(\alpha)$) has d roots inside the unit disk $|\alpha| < 1$. We denote them by α_j^+ (resp. α_j^-), $j = 1, \dots d$. Let $M_{\text{ad}}^+(\alpha)$ be the matrix of cofactors of $M_+(\alpha)$ and $M_{\text{ad}}^-(\alpha)$ the one associated with $M_-(\alpha)$ and let q_j^+ (resp. q_j^-) be a non-zero column of $M_{\text{ad}}^+(\alpha_j^+)$ (resp. $M_{\text{ad}}^-(\alpha_j^-)$).

> *We assume that the* α_j^+ *(resp.* α_j^-*) are all distinct. Then a solution basis is*
>
> $$\begin{aligned} \varphi_j(\nu, \theta) &= e^{-i\theta\nu}(\alpha_j^+ e^{2i\theta} + 1)^\nu q_j^+, \ j = 1, \dots d, \\ \varphi_{j+d}(\nu, \theta) &= e^{i\theta\nu}(\alpha_j^- e^{-2i\theta} + 1)^\nu q_j^-, \ j = 1, \dots d. \end{aligned}$$

Remark. The roots α_j^+ (resp. α_j^-) are generically all distinct when the material is anisotropic. If some of them coincide, there still exists an explicit formulation based on Cauchy integrals (given in [2]). We do not treat here the case when the material is anisotropic and some roots coincide, since it corresponds to a quite rare situation, highly depending on the accuracy of the data.

However, an important particular case is the isotropic one, where the roots α_j are all equal to zero. One can find an explicit formulation of the solution basis in several papers, for instance in [4] and [8]. In cartesian coordinates, a solution basis in the isotropic case is given by

- in dimension 2 :

$$\varphi_1(\nu,\theta) = \begin{pmatrix} \cos(\theta\nu) \\ -\sin(\theta\nu) \end{pmatrix}, \quad \varphi_2(\nu,\theta) = \begin{pmatrix} \sin(\theta\nu) \\ \cos(\theta\nu) \end{pmatrix},$$

$$\varphi_3(\nu,\theta) = \begin{pmatrix} (\lambda+3\mu)\cos(\theta\nu) \\ (\lambda+3\mu)\sin(\theta\nu) \end{pmatrix} + \nu\psi_2(\nu,\theta), \quad \varphi_4(\nu,\theta) = \begin{pmatrix} -(\lambda+3\mu)\sin(\theta\nu) \\ (\lambda+3\mu)\cos(\theta\nu) \end{pmatrix} + \nu\psi_1(\nu,\theta),$$

$$\text{where} \quad \psi_1(\nu,\theta) = \begin{pmatrix} (\lambda+\mu)\sin\big(\theta(\nu-2)\big) \\ (\lambda+\mu)\cos\big(\theta(\nu-2)\big) \end{pmatrix} \quad \text{and} \quad \psi_2(\nu,\theta) = \begin{pmatrix} -(\lambda+\mu)\cos\big(\theta(\nu-2)\big) \\ (\lambda+\mu)\sin\big(\theta(\nu-2)\big) \end{pmatrix}.$$

- in dimension 3, the third equation of the system is a Laplace equation uncoupled from the others. The six basis functions are then given by the four previous ones with a zero third component, plus

$$\varphi_5(\nu,\theta) = \begin{pmatrix} 0 \\ 0 \\ \sin(\theta\nu) \end{pmatrix}, \quad \varphi_6(\nu,\theta) = \begin{pmatrix} 0 \\ 0 \\ \cos(\theta\nu) \end{pmatrix}.$$

3. Expression of the elasticity system

Notation. In the following, we write ∂_k instead of ∂x_k.

The system L comes from the application of the laws of mechanics in the case of linear elasticity and depends on the classical quantities :

. displacement field $u = (u_1, \dots u_d)$,
. strain tensor $\varepsilon_{kl}(u) = \frac{1}{2}(\partial_k u_l + \partial_l u_k)$,
. stress tensor $\sigma_{ij}(u) = \sum_{kl} a_{ijkl}\, \varepsilon_{kl}(u)$, where a_{ijkl} are elasticity constants satisfying the following symmetry properties

$$a_{ijkl} = a_{jikl} = a_{ijlk} = a_{klij}.$$

The general equilibrium equation is

$$Lu = f \qquad \text{where} \qquad (Lu)_i = -\sum_j \partial_j \sigma_{ij}(u),$$

or, taking into account the previous definitions and properties

$$-\frac{1}{2}\sum_{jkl} a_{ijkl}\ \partial_j(\partial_k u_l + \partial_l u_k) = f_i. \tag{4}$$

To simplify the expressions, a common practice is to change the name of the coefficients by setting $c_{pq} = a_{ijkl}$, according to the following numbering convention which takes into account the symmetries :

p, q	1	2	3	4	5	6
ij, kl	11	22	33	23	13	12

Each index i, j, k, l varies in $\{1, \dots d\}$. From the definition (§ **2.1**), the reduced operator M associated to the system (4) is then

- in dimension 2,

$$\begin{cases} \big[c_{11}\partial_1^2 + 2c_{16}\partial_1\partial_2 + c_{66}\partial_2^2\big]u_1 + \big[c_{16}\partial_1^2 + (c_{12}+c_{66})\partial_1\partial_2 + c_{26}\partial_2^2\big]u_2 \\ \big[c_{16}\partial_1^2 + (c_{12}+c_{66})\partial_1\partial_2 + c_{26}\partial_2^2\big]u_1 + \big[c_{66}\partial_1^2 + 2c_{26}\partial_1\partial_2 + c_{22}\partial_2^2\big]u_2 \end{cases}$$

- in dimension 3 (with $z = x_3$ the coordinate along the edge),

$$\begin{cases} \big[c_{11}\partial_1^2 + 2c_{16}\partial_1\partial_2 + c_{66}\partial_2^2\big]u_1 + \big[c_{16}\partial_1^2 + (c_{12}+c_{66})\partial_1\partial_2 + c_{26}\partial_2^2\big]u_2 + \\ \qquad\qquad \big[c_{15}\partial_1^2 + (c_{14}+c_{56})\partial_1\partial_2 + c_{46}\partial_2^2\big]u_3 \\ \big[c_{16}\partial_1^2 + (c_{12}+c_{66})\partial_1\partial_2 + c_{26}\partial_2^2\big]u_1 + \big[c_{66}\partial_1^2 + 2c_{26}\partial_1\partial_2 + c_{22}\partial_2^2\big]u_2 + \\ \qquad\qquad \big[c_{56}\partial_1^2 + (c_{25}+c_{46})\partial_1\partial_2 + c_{24}\partial_2^2\big]u_3 \\ \big[c_{15}\partial_1^2 + (c_{14}+c_{56})\partial_1\partial_2 + c_{46}\partial_2^2\big]u_1 + \big[c_{56}\partial_1^2 + (c_{25}+c_{46})\partial_1\partial_2 + c_{24}\partial_2^2\big]u_2 + \\ \qquad\qquad \big[c_{55}\partial_1^2 + 2c_{45}\partial_1\partial_2 + c_{44}\partial_2^2\big]u_3 \end{cases}$$

4. Characteristic determinant

We already know a solution basis of the homogeneous problem without boundary or transmission conditions. To compute the singularity exponents, we have now to take them into account.

4.1 Dirichlet and Neumann conditions

Given the normal vector $\vec{n} = (n_1, \dots n_d)$ at a point on the boundary $\partial\Omega$ of the domain, the normal stress vector is defined by $\sigma(u)\vec{n}$.

There are essentially two kinds of boundary conditions :

$$\begin{array}{ll} \text{Dirichlet condition} & : \quad u = 0, \\ \text{Neumann condition} & : \quad \sigma(u)\vec{n} = 0. \end{array}$$

Dirichlet conditions are straightforward. Neumann conditions need however to be expressed precisely. In particular, in dimension 3, the "reduced" normal stress $\vec{T}(u)$, where the tangential derivative ∂_3 along the edge has to removed, has to be used.

The components of vector $\vec{T}(u)$ are the following :

- normal stress $\vec{T}(u) = \sigma(u)\vec{n}$ in dimension 2

$$\left| \begin{array}{l} \big[c_{11}\partial_1 u_1 + c_{16}(\partial_1 u_2 + \partial_2 u_1) + c_{12}\partial_2 u_2\big]n_1 + \big[c_{16}\partial_1 u_1 + c_{66}(\partial_1 u_2 + \partial_2 u_1) + c_{26}\partial_2 u_2\big]n_2 \\ \big[c_{16}\partial_1 u_1 + c_{66}(\partial_1 u_2 + \partial_2 u_1) + c_{26}\partial_2 u_2\big]n_1 + \big[c_{12}\partial_1 u_1 + c_{26}(\partial_1 u_2 + \partial_2 u_1) + c_{22}\partial_2 u_2\big]n_2 \end{array} \right.$$

- reduced normal stress $\vec{T}(u)$ in dimension 3 (considering the definition of the axes, the third component n_3 of the normal vector is zero)

$$\left| \begin{array}{l} \big[c_{11}\partial_1 u_1 + c_{16}(\partial_1 u_2 + \partial_2 u_1) + c_{15}\partial_1 u_3 + c_{12}\partial_2 u_2 + c_{14}\partial_2 u_3\big]n_1 + \\ \big[c_{16}\partial_1 u_1 + c_{66}(\partial_1 u_2 + \partial_2 u_1) + c_{56}\partial_1 u_3 + c_{26}\partial_2 u_2 + c_{46}\partial_2 u_3\big]n_2 \\ \big[c_{16}\partial_1 u_1 + c_{66}(\partial_1 u_2 + \partial_2 u_1) + c_{56}\partial_1 u_3 + c_{26}\partial_2 u_2 + c_{46}\partial_2 u_3\big]n_1 + \\ \big[c_{12}\partial_1 u_1 + c_{26}(\partial_1 u_2 + \partial_2 u_1) + c_{25}\partial_1 u_3 + c_{22}\partial_2 u_2 + c_{24}\partial_2 u_3\big]n_2 \\ \big[c_{15}\partial_1 u_1 + c_{56}(\partial_1 u_2 + \partial_2 u_1) + c_{55}\partial_1 u_3 + c_{25}\partial_2 u_2 + c_{45}\partial_2 u_3\big]n_1 + \\ \big[c_{14}\partial_1 u_1 + c_{46}(\partial_1 u_2 + \partial_2 u_1) + c_{45}\partial_1 u_3 + c_{24}\partial_2 u_2 + c_{44}\partial_2 u_3\big]n_2 \end{array} \right.$$

4.2 Construction of the boundary condition matrix

We consider the general situation of a transmission problem between several materials, each of them in one domain Ω_k. Let $\mathcal{O}$ be the corner of a Ω_k in dimension 2, or a point in one edge of a Ω_k in dimension 3. After a possible renumbering, let $\Omega_1, \ldots, \Omega_K$ be the domains containing $\mathcal{O}$ in their boundaries. In dimension 2, tangents at the boundaries in this point define angular sectors Γ_k lying between angles ω_{k-1} and ω_k. In dimension 3, we cut Ω by the plane perpendicular to the edge containing $\mathcal{O}$ and we are reduced to the previous geometry, which allows for the definition of Γ_k and ω_k.

Let M_k be the reduced operator associated with the system L_k in the domain Ω_k. The singularity exponents ν and the associated angular functions g at $\mathcal{O}$ for the problem

$$\begin{cases} L_k u = f \ \text{ in } \Omega_k, \\ \text{Transmission conditions on } \partial\Omega_k \setminus \partial\Omega, \\ \text{Boundary conditions on } \partial\Omega, \end{cases} \tag{5}$$

are the complex numbers ν and the non-zero functions $g : (\omega_0, \omega_K) \longmapsto \mathbb{C}^d$ solution of the problem

$$\begin{cases} M_k\big(r^\nu g(\theta)\big) = 0 \ \text{ in } (\omega_{k-1}, \omega_k), \quad k = 1, \ldots, K, \\ \text{Transmission conditions on } \omega_k,\ k = 1 \ldots, K-1. \\ \text{Zero boundary conditions on } \omega_0 \text{ and } \omega_K. \end{cases} \tag{6}$$

Any solution (ν, g) of (6) is such that for any k, the restriction g_k of g to (ω_{k-1}, ω_k) belongs to the space generated by the $\varphi_j^{(k)}(\nu)$, thus there exist coefficients $z_j^{(k)}$ such that

$$g_k = \sum_{j=1}^{2d} z_j^{(k)} \varphi_j^{(k)}(\nu), \quad k = 1, \ldots, K. \tag{7}$$

Thus, to solve (6), we have to find all non-zero set of coefficients $z_j^{(k)}$, $j = 1, \ldots, 2d$, $k = 1, \ldots, K$, satisfying the conditions

$$\begin{cases} \text{Boundary conditions in } \omega_0 \\ \begin{aligned} \textstyle\sum_{j=1}^{2d} z_j^{(1)} r^\nu \varphi_j^{(1)}(\nu)(\omega_1) - \sum_{j=1}^{2d} z_j^{(2)} r^\nu \varphi_j^{(2)}(\nu)(\omega_1) &= 0 \\ \textstyle\sum_{j=1}^{2d} z_j^{(1)} \vec{T}\big(r^\nu \varphi_j^{(1)}(\nu)\big)(\omega_1) - \sum_{j=1}^{2d} z_j^{(2)} \vec{T}\big(r^\nu \varphi_j^{(2)}(\nu)\big)(\omega_1) &= 0 \\ \vdots & \\ \textstyle\sum_{j=1}^{2d} z_j^{(K-1)} r^\nu \varphi_j^{(K-1)}(\nu)(\omega_{K-1}) - \sum_{j=1}^{2d} z_j^{(K)} r^\nu \varphi_j^{(K)}(\nu)(\omega_{K-1}) &= 0 \\ \textstyle\sum_{j=1}^{2d} z_j^{(K-1)} \vec{T}\big(r^\nu \varphi_j^{(K-1)}(\nu)\big)(\omega_{K-1}) - \sum_{j=1}^{2d} z_j^{(K)} \vec{T}\big(r^\nu \varphi_j^{(K)}(\nu)\big)(\omega_{K-1}) &= 0 \end{aligned} \\ \text{Boundary conditions in } \omega_K \end{cases}$$

which ensure the boundary and transmission conditions for the function g defined by (7).

As the functions involved are homogeneous of degree ν or $\nu - 1$ in r, it suffices that the above equalities hold for $r = 1$. This can be expressed as a system $A(\nu)z = 0$ with $z \in \mathbb{C}^{2dK}$ and $A(\nu)$ the *characteristic matrix* given below. It admits a non-zero solution if $A(\nu)$ is not invertible. So, singularity exponents ν can be computed as solutions of the equation $\det A(\nu) = 0$.

We denote by :

- $\Phi^{(k)}(\nu)$ the set of basis solutions $\{\varphi_j^{(k)}(\nu, \theta), j = 1, \ldots 2d\}$ associated with M_k, whose expressions are given in § **2.2**,

- $D_{\theta_0}\Phi(\nu) = \big(\varphi_1(\nu,\theta_0),\dots,\varphi_{2d}(\nu,\theta_0)\big)$ the trace of Dirichlet boundary conditions along the line $\theta=\theta_0$ for the solution basis Φ,
- $N^{(k)}_{\theta_0}\Phi(\nu) = \big(\vec{T}(r^\nu\varphi_1(\nu,\theta_0))|_{r=1},\dots,\vec{T}(r^\nu\varphi_{2d}(\nu,\theta_0))|_{r=1}\big)$ the trace of Neumann boundary conditions associated with M_k along the line $\theta=\theta_0$ for the solution basis Φ.

With the above notations, the *characteristic matrix* $A(\nu)$ is the $2dK\times 2dK$ matrix built by blocks in the following manner, each block X, $D\Phi$ or $N\Phi$ being of dimension $(d,2d)$:

$$A(\nu)=\begin{pmatrix}
X_{1,1} & 0 & 0 & 0 & \dots & X_{1,K}\\
D_{\omega_1}\Phi^{(1)}(\nu) & -D_{\omega_1}\Phi^{(2)}(\nu) & 0 & 0 & \dots & 0\\
N^{(1)}_{\omega_1}\Phi^{(1)}(\nu) & -N^{(2)}_{\omega_1}\Phi^{(2)}(\nu) & 0 & 0 & \dots & 0\\
0 & D_{\omega_2}\Phi^{(2)}(\nu) & -D_{\omega_2}\Phi^{(3)}(\nu) & 0 & \dots & 0\\
0 & N^{(2)}_{\omega_2}\Phi^{(2)}(\nu) & -N^{(3)}_{\omega_2}\Phi^{(3)}(\nu) & 0 & \dots & 0\\
0 & 0 & D_{\omega_3}\Phi^{(3)}(\nu) & \ddots & & 0\\
0 & 0 & N^{(3)}_{\omega_3}\Phi^{(3)}(\nu) & \ddots & & 0\\
0 & 0 & 0 & \ddots & & 0\\
\vdots & \vdots & \vdots & \ddots & \ddots & \vdots\\
0 & 0 & 0 & 0 & \ddots & -D_{\omega_{K-1}}\Phi^{(K)}(\nu)\\
0 & 0 & 0 & 0 & \ddots & -N^{(K)}_{\omega_{K-1}}\Phi^{(K)}(\nu)\\
X_{2K,1} & 0 & 0 & 0 & \dots & X_{2K,K}
\end{pmatrix}$$

It remains to describe explicitly the boundary blocks $X_{1,1}$, $X_{1,K}$, $X_{2K,1}$ and $X_{2K,K}$.

4.3 General boundary conditions

There are two situations.

4.3.i *Case of an interior point.*

This is the situation when $\mathcal{O}$ belongs to the interior of the domain Ω. This means that $\mathcal{O}$ is an interior transmission point. Then $\omega_K=\omega_0+2\pi$ and all the domains are filling the space. The boundary operators X are

$$X_{1,1}=D_{\omega_0}\Phi^{(1)}(\nu),\qquad X_{1,K}=-D_{\omega_K}\Phi^{(K)}(\nu),$$
$$X_{2K,1}=N^{(1)}_{\omega_0}\Phi^{(1)}(\nu),\quad X_{2K,K}=-N^{(K)}_{\omega_K}\Phi^{(K)}(\nu).$$

4.3.ii *Case of an exterior point.*

This is the situation when $\mathcal{O}$ belongs to the boundary of the domain Ω. Thus boundary conditions are imposed on the boundary angles ω_0 and ω_K. We always have $X_{2K,1}=X_{1,K}=0$, and according to boundary conditions that are chosen, we have

- Dirichlet conditions :

$$X_{1,1}=D_{\omega_0}\Phi^{(1)}(\nu),\qquad X_{2K,K}=D_{\omega_K}\Phi^{(K)}(\nu)$$

- Neumann conditions :

$$X_{1,1}=N^{(1)}_{\omega_0}\Phi^{(1)}(\nu),\qquad X_{2K,K}=N^{(K)}_{\omega_K}\Phi^{(K)}(\nu).$$

It is possible to take into account mixed boundary conditions, such as Dirichlet along a boundary and Neumann along the other. We can also treat other types of mixed conditions : we mention *normal Dirichlet – tangent Neumann* and *tangent Dirichlet – normal Neumann*. For their introduction, let us use the general vector notation $\vec{u}$ for each function $r^\nu \varphi_j(\nu,\theta)$.

In dimension 2, we consider the orthonormal basis $(\vec{n},\vec{t})$, deduced from $(\vec{x_1},\vec{x_2})$ by a rotation, and we write the boundary conditions in this basis :

- normal Dirichlet – tangent Neumann

$$\begin{array}{ll} 1^{\text{st}} \text{ component :} & \vec{u}\cdot\vec{n}=0 \\ 2^{\text{nd}} \text{ component :} & \vec{T}(\vec{u})\cdot\vec{t}=0 \end{array}$$

- tangent Dirichlet – normal Neumann

$$\begin{array}{ll} 1^{\text{st}} \text{ component :} & \vec{u}\cdot\vec{t}=0 \\ 2^{\text{nd}} \text{ component :} & \vec{T}(\vec{u})\cdot\vec{n}=0 \end{array}$$

In dimension 3, we consider the orthonormal basis $(\vec{n},\vec{t},\vec{z})$, deduced from the local basis $(\vec{x},\vec{y},\vec{z})$ by a rotation around $\vec{z}$. The direction $\vec{z}$ is, by definition, a tangent direction, so we have here one normal direction $\vec{n}$ and two tangent directions $\vec{t}$ and $\vec{z}$.

To the previous components, where $\vec{x_3}$ stands for $\vec{z}$, we then have to add

- Dirichlet tangent : $\vec{u}\cdot\vec{z}=0$
- Neumann tangent : $\vec{T}(\vec{u})\cdot\vec{z}=0$

5. Computation of the characteristic matrix

We describe here the computational aspects of the determination of the matrix $A(\nu)$.

5.1 Roots of the determinant of the symbol

We recall that, for each non isotropic material, the solution basis given in § **2.2** involves the computation of α_j^+ and α_j^-, roots of $\det M_+(\alpha)$ and $\det M_-(\alpha)$.

5.1.i *General case.*

Let $\xi \in \mathbb{R}$ and let us consider the symbol $M(1,\xi)$. Note that $\det M(1,\xi)$ is a polynomial of degree $2d$ in ξ with real coefficients. There holds

> *The roots α_j^+ are given by*
>
> $$\alpha_j^+ = \mathcal{A}(\beta_j) \stackrel{\text{def}}{=} \frac{i+\beta_j}{i-\beta_j}$$
>
> *where the β_j, $j=1,\dots,d$ are the roots of $\det M(1,\xi)$ of negative imaginary part. The roots α_j^- are equal to the conjugates $\overline{\alpha_j^+}$.*

Indeed, let β be one of the roots of $\det M(1,\xi)$. Then for $\alpha=\mathcal{A}(\beta)$, β is the Cayley transform

$$\beta = \mathcal{B}(\alpha) \stackrel{\text{def}}{=} \frac{i(\alpha-1)}{\alpha+1}$$

of α. Then, since $\det M(1,\beta) = (\alpha+1)^{-d} \det M_+(\alpha)$, α is a root of $\det M_+(\alpha)$. Moreover, writing $\alpha=\rho e^{i\theta}$, we get

$$\beta = \frac{-2\rho\sin\theta + i(\rho^2-1)}{(\rho+\cos\theta)^2+\sin^2\theta}$$

so that $|\alpha|<1 \Longleftrightarrow \operatorname{Im}\beta<0$.

In the same way, for $\alpha = \overline{\mathcal{A}(\overline{\beta})}$, there holds $\beta = -\mathcal{B}(\alpha)$, and α is root of $\det M_-(\alpha)$. Moreover $|\alpha| < 1 \Longleftrightarrow \operatorname{Im}\beta > 0$. Finally, if β is a root of $\det M(1,\xi)$, then $\overline{\beta}$ is also a root since M is real.

Thus, it is sufficient to compute the roots of $\det M(1,\xi)$ with negative imaginary part. From a computational point of view, using $\det M(1,\xi)$ is more efficient than using directly $\det M_+(\alpha)$ because its coefficients are real : we can expect a better accuracy.

Several methods can be used to compute the roots of this polynomial. We chose Bairstow's method, which is based on a factorization of the polynomial into a product of polynomials of degree 2 using Newton–Raphson's method. We finally use Newton's method on the original polynomial to get more accuracy on each root.

5.1.ii *Orthotropic axisymmetric case in dimension 2.*

Here, the roots of the symbol can be computed explicitly. In the case of an orthotropic system, we have $c_{16} = c_{26} = 0$. The matrices $M_+(\alpha)$ and $M_-(\alpha)$ are then

$$M_+(\alpha) = \begin{pmatrix} (c_{11}-c_{66})(\alpha^2+1)+2(c_{11}+c_{66})\alpha & i(c_{12}+c_{66})(\alpha^2-1) \\ i(c_{12}+c_{66})(\alpha^2-1) & (c_{66}-c_{22})(\alpha^2+1)+2(c_{66}+c_{22})\alpha \end{pmatrix}$$

and

$$M_-(\alpha) = \begin{pmatrix} (c_{11}-c_{66})(\alpha^2+1)+2(c_{11}+c_{66})\alpha & -i(c_{12}+c_{66})(\alpha^2-1) \\ -i(c_{12}+c_{66})(\alpha^2-1) & (c_{66}-c_{22})(\alpha^2+1)+2(c_{66}+c_{22})\alpha \end{pmatrix}.$$

In the orthotropic axisymmetric case, we have also $c_{11} = c_{22}$. Setting $c_{11} = c_{22} = \kappa_1$, $c_{66} = \kappa_6$ and $c_{12} + c_{66} = \gamma$, the determinant can be written

$$D = [\gamma^2 - (\kappa_1 - \kappa_6)^2]\alpha^4 + 2(\kappa_1^2 + 6\kappa_1\kappa_6 + \kappa_6^2 - \gamma^2)\alpha^2 + [\gamma^2 - (\kappa_1 - \kappa_6)^2].$$

$$D = 0 \Longleftrightarrow \alpha^4 - 2b\alpha^2 + 1 = 0 \quad \text{with} \quad b = 1 + \frac{8\kappa_1\kappa_6}{(\kappa_1-\kappa_6)^2 - \gamma^2}.$$

The discriminant of this equation is $\Delta = b^2 - 1$ and $\Delta > 0$. Indeed, assume $|b| < 1$. We then have $\alpha^2 = b \pm i\sqrt{1-b^2}$, so $|\alpha^2| = 1$, which contradicts the ellipticity hypothesis ensuring that 2 roots are inside the unit disk and 2 roots outside.

Thus, we have $\alpha^2 = b \pm \sqrt{\Delta}$ and we look for roots of minimum modulus. Using the fact that $|b| > 1$ implies $|b| > \sqrt{\Delta}$, we get :

- if $b > 0$, $\alpha = \pm\sqrt{b - \sqrt{\Delta}}$
- if $b < 0$, $\alpha = \pm i\sqrt{-b - \sqrt{\Delta}}$.

5.2 Solution basis

The solution basis is computed using the formulas given in § **2.2**. This involves the computation of the matrix of cofactors and then the extraction of the vectors q^+ and q^-.

As the coefficients of the matrix M are real, there holds

$$M^-_{\mathrm{ad}}(\overline{\alpha}) = \overline{M^+_{\mathrm{ad}}(\alpha)} \quad \text{and} \quad q^- = \overline{q^+}.$$

So it is sufficient to compute vectors q^+ which we normalize in order to ensure stability of the numerical computations.

5.3 Applying Neumann conditions to the solution basis

In the equations given in § **4.1**, $u = (u_1, \dots u_d)$ is successively replaced by every function $r^\nu \varphi_j(\nu), j = 1, \dots 2d$, where $\varphi_j(\nu) = \big(\varphi_{j,1}(\nu), \dots \varphi_{j,d}(\nu)\big)$ is one element of the solution basis given in § **2.2**. To calculate $\partial_i u$, we then need to use polar coordinates.

With $(n_1, n_2) = (-\sin\theta, \cos\theta)$, we get for $r^\nu \varphi_j(\nu)$:

$$\begin{cases} \partial_1\big(r^\nu \varphi_j(\nu)\big) &= r^{\nu-1}\big(n_2\, \nu\, \varphi_j(\nu) + n_1\, \partial_\theta \varphi_j(\nu)\big) \\ \partial_2\big(r^\nu \varphi_j(\nu)\big) &= r^{\nu-1}\big(-n_1\, \nu\, \varphi_j(\nu) + n_2\, \partial_\theta \varphi_j(\nu)\big) \end{cases}$$

The last term to describe is $\partial_\theta \varphi_j(\nu)$.

5.3.i *Non isotropic case.*

Let $\gamma = \alpha_j^+ e^{2i\theta}$ and $\beta = i(\gamma - 1)$. Recalling that $\alpha_j^- = \overline{\alpha_j^+}$ and $q_j^- = \overline{q_j^+}$, we have for $j = 1, \dots d$

$$\begin{aligned} \partial_\theta \varphi_j(\nu, \theta) &= \beta\nu\ e^{-i\theta\nu}(\gamma + 1)^{\nu-1} q_j^+, \\ \partial_\theta \varphi_{j+d}(\nu, \theta) &= \overline{\beta}\nu\ e^{i\theta\nu}(\overline{\gamma} + 1)^{\nu-1}\ \overline{q_j^+}. \end{aligned}$$

5.3.ii *Isotropic case.*

We have

$$\partial_\theta \varphi_1(\nu,\theta) = -\nu\varphi_2(\nu,\theta), \quad \partial_\theta \varphi_2(\nu,\theta) = \nu\varphi_1(\nu,\theta), \quad \partial_\theta \varphi_3(\nu,\theta) = \nu(\varphi_4 - 2\psi_1)(\nu,\theta),$$
$$\partial_\theta \varphi_4(\nu,\theta) = \nu(-\varphi_3 + 2\psi_2)(\nu,\theta), \quad \partial_\theta \varphi_5(\nu,\theta) = \nu\varphi_6(\nu,\theta), \quad \partial_\theta \varphi_6(\nu,\theta) = -\nu\varphi_5(\nu,\theta),$$

where ψ_1 and ψ_2 are defined in § **2.2**.

Thus we have all elements for the construction of the blocks $D_\omega \Phi(\nu)$ and $N_\omega^{(k)} \Phi(\nu)$.

6. Computation of singularity exponents

6.1 Numerical aspect

Singularity exponents are the roots of the equation $\det A(\nu) = 0$. To compute this determinant, we make an LU decomposition of $A(\nu)$.

The next problem is to locate the roots. For that purpose, we use Cauchy integrals over closed curves. Given holomorphic functions f and g and a closed simple contour C, Cauchy's formula is

$$\frac{1}{2i\pi} \int_C g(\nu) \frac{f'(\nu)}{f(\nu)}\, d\nu = \sum_{\rho \in S} g(\rho)$$

where S is the set of the roots of f in the interior of C. Taking $g(\nu) = 1$, we can compute the number of roots inside the curve and thus isolate each root, which we then compute with $g(\nu) = \nu$.

We use this formula with $f(\nu) = \det A(\nu)$. In our code, the curves used are rectangles or circles. The quadrature method chosen is Simpson's rule over a rectangle and trapezium rule over a circle. The computation of the integrand is crucial. Here, we take advantage of the particular form of the function f. Thus, we have

$$\frac{f'(\nu)}{f(\nu)} = \mathrm{tr}\big(A'(\nu) A^{-1}(\nu)\big),$$

where $\mathrm{tr}(M)$ is the trace of the matrix M and $A'(\nu)$ the matrix $A(\nu)$ derived element by element with respect to ν.

The computation of $A'(\nu)$ is explicit (see below) ; so only the non-zero elements are computed, with the maximum precision possible. Moreover, $A'(\nu)$ is computed at the same time as $A(\nu)$ reusing several intermediate calculations.

6.2 Computation of the derived matrix

We already defined $\gamma = \alpha_j^+ e^{2i\theta}$ and $\beta = i(\gamma - 1)$. Moreover, let δ be defined as $\delta = \log(\gamma+1) - i\theta$.

To compute the matrix $A'(\nu)$ we need the derivatives of each element of $A(\nu)$ with respect to ν. Thus, we have to compute terms such as $\partial_\nu(D_\theta\Phi)$ and $\partial_\nu(N_\theta^{(k)}\Phi)$, i.e. $\partial_\nu(\varphi_j(\nu))$ and $\partial_\nu\big(\vec{T}(r^\nu\varphi_j(\nu))|_{r=1}\big)$.

6.2.i *Non isotropic case.*

From the definition of the solution basis, we get, for $j = 1, \dots d$:

$$\begin{aligned} \partial_\nu\varphi_j(\nu,\theta) &= \delta\ \varphi_j(\nu,\theta), \\ \partial_\nu\varphi_{j+d}(\nu,\theta) &= \overline{\delta}\ \varphi_{j+d}(\nu,\theta). \end{aligned}$$

As for Neumann conditions, the gradient vector used in the computations can be written as

$$R\begin{pmatrix} \nu\varphi_j(\nu,\theta) \\ \partial_\theta\varphi_j(\nu,\theta) \end{pmatrix} \quad \text{with} \quad R = \begin{pmatrix} n_2 & n_1 \\ -n_1 & n_2 \end{pmatrix}.$$

After derivation with respect to ν, we get

$$R\begin{pmatrix} \varphi_j(\nu,\theta) + \nu\ \partial_\nu\varphi_j(\nu,\theta) \\ \partial_\nu\big(\partial_\theta\varphi_j(\nu,\theta)\big) \end{pmatrix}.$$

It remains to write the last component, which is for $j = 1, \dots d$:

$$\begin{aligned} \partial_\nu\partial_\theta\varphi_j(\nu,\theta) &= \tfrac{(1+\nu\delta)}{\nu}\ \partial_\theta\varphi_j(\nu,\theta), \\ \partial_\nu\partial_\theta\varphi_{j+d}(\nu,\theta) &= \tfrac{(1+\nu\overline{\delta})}{\nu}\ \partial_\theta\varphi_{j+d}(\nu,\theta). \end{aligned}$$

6.2.ii *Isotropic case.*

We have

$$\partial_\nu\varphi_1(\nu,\theta) = -\theta\varphi_2(\nu,\theta), \quad \partial_\nu\varphi_2(\nu,\theta) = \theta\varphi_1(\nu,\theta), \quad \partial_\nu\varphi_3(\nu,\theta) = (\theta\varphi_4 + \psi_2)(\nu,\theta),$$
$$\partial_\nu\varphi_4(\nu,\theta) = (-\theta\varphi_3 + \psi_1)(\nu,\theta), \quad \partial_\nu\varphi_5(\nu,\theta) = \theta\varphi_6(\nu,\theta), \quad \partial_\nu\varphi_6(\nu,\theta) = -\theta\varphi_5(\nu,\theta),$$

and

$$\partial_\nu\partial_\theta\varphi_1(\nu,\theta) = (-\varphi_2 - \theta\nu\varphi_1)(\nu,\theta), \quad \partial_\nu\partial_\theta\varphi_2(\nu,\theta) = (\varphi_1 - \theta\nu\varphi_2)(\nu,\theta),$$
$$\partial_\nu\partial_\theta\varphi_3(\nu,\theta) = (\varphi_4 + \theta\partial_\theta\varphi_4 + (\nu-2)\psi_1)(\nu,\theta), \quad \partial_\nu\partial_\theta\varphi_4(\nu,\theta) = (-\varphi_3 - \theta\partial_\theta\varphi_3 - (\nu-2)\psi_2)(\nu,\theta),$$
$$\partial_\nu\partial_\theta\varphi_5(\nu,\theta) = (\varphi_6 + \nu\partial_\nu\varphi_6)(\nu,\theta), \quad \partial_\nu\partial_\theta\varphi_6(\nu,\theta) = (-\varphi_5 - \nu\partial_\nu\varphi_5)(\nu,\theta),$$

where ψ_1 and ψ_2 are defined in § **2.2**.

6.3 Algorithmic aspect

With our program, the search of the roots can be done manually, or automatically in a given rectangular domain of the complex plane.

In the automatic case, many tests have been performed to devise an efficient method. They led to an iterative method based on successive splits of the initial domain into smaller and smaller rectangles in order to isolate a root. Given a predefined tolerance ε, an estimation $\nu^{(n)}$ of ν satisfying $|\nu^{(n)} - \nu^{(n-1)}| < \varepsilon$ is then computed, using successive integrals over circles.

Provided a good idea of the location of the roots, one can significantly reduce the time devoted to the splitting phase. Indeed, what is of practical interest is often to study problems depending continuously on a parameter. We use the fact that the location of the exponents also varies

continuously with respect to this parameter as a partial information to find the exponents at the next step. Obviously, if the step size is too large, this additional information is not helpful and then ignored.

7. Computation of singular functions

Let $\widetilde{\varphi}_j^{(k)}(\nu,\theta)$ be defined as $\varphi_j^{(k)}(\nu,\theta)$ for $\theta \in (\omega_{k-1},\omega_k)$ and by 0 for $\theta \in (\omega_0,\omega_K) \setminus (\omega_{k-1},\omega_k)$. A singularity exponent ν is solution of the equation $\det A(\nu) = 0$, that is to say there exists a non zero linear combination, *cf* (7),

$$g(\theta) = \sum_{k=1}^{K} \sum_{j=1}^{2d} z_j^{(k)} \widetilde{\varphi}_j^{(k)}(\nu,\theta),$$

solution of the homogeneous problem with boundary conditions (6) : any such function is an angular singular function associated with the singularity exponent ν.

Coefficients $z_j^{(k)}$ are the components of a vector z lying in $\ker A(\nu)$. In order to exhibit such a vector, a method consists in computing the singular value decomposition of $A(\nu)$. We then have $A(\nu) = USV^*$ where U and V are two unitary matrices and S a diagonal matrix containing the singular values of $A(\nu)$. This decomposition is quite adapted to our purpose since it turns out that, if the singular value s_{ii} is null, then the i-th column vector of V is in $\ker A(\nu)$.

In general, the dimension of $\ker A(\nu)$ is equal to the multiplicity of ν, considered as the root of the analytic function $\det A(\nu)$. In this case, the method is able to completely determine the singular functions. The accuracy on ν is essential in order to correctly separate the singular values and thus select the right vectors in the matrix V.

However, it can happen that the dimension of the kernel is less than the multiplicity of the singularity exponent ν. Then, logarithmic terms appear in the asymptotic expansion of u_{sing} in the form $B_0\, r^\nu g_0(\theta) + B_1\, r^\nu (g_1(\theta) + \ln r\, g_0(\theta)) + \cdots$, where $(g_0, g_1, \ldots)$ forms a Jordan chain. In this case, singular functions are not necessarily in $\ker A(\nu)$ and cannot be computed directly with this method. This situation is easily detected by comparing the multiplicity of the exponent with the dimension of the kernel.

8. Case of a three dimensional domain

We know that in a point $\mathcal{O}$ lying on an edge, singularity exponents do not depend on tangential derivatives ∂_z. Thus, the problem remains bidimensional in the plane $(\mathcal{O};\vec{x},\vec{y})$. Computing singularity exponents in other points of the edge means to move the local axes along the edge and the coefficients of rigidity matrices in the local basis, because, except for isotropic material, those coefficients depend on the basis used.

Each material is assumed to be homogeneous, so coefficients are invariant under translation. Then given two orthonormal basis B and B', we consider a rotation R whose matrix is defined by $R = [R(B)]_B = [B']_B$. We know the coefficients in B and are looking for them in B'.

Let us denote by σ and ε, (resp. σ' and ε') the stress tensor and the strain tensor written in B (resp. B'). Then we have $\sigma' = R^T \sigma R$ and $\varepsilon' = R^T \varepsilon R$. Since in B coefficients are characterized by the relation $\sigma_{ij} = a_{ijkl}\, \varepsilon_{kl}$ (to simplify the expressions, we use the summation convention upon identical indices in an expression), coefficients a' used in B' can be deduced from $\sigma'_{i'j'} = R^T_{i'i}\, \sigma_{ij}\, R_{jj'} = R_{ii'}\, R_{jj'}\, a_{ijkl}\, \varepsilon_{kl}$.

We then have $\sigma'_{i'j'} = a'_{i'j'k'l'}\, \varepsilon'_{k'l'}$ where $a'_{i'j'k'l'} = R_{ii'}\, R_{jj'}\, R_{kk'}\, R_{ll'}\, a_{ijkl}$.

9. Examples

In this part, we illustrate the efficiency of the method. We compare with known results, focusing on some interesting details. At last, we propose a typical example of our own, showing what is easy to obtain in dimension 3.

All the computations have been done on a DEC Alpha workstation using double precision arithmetic. The tolerance ε has been set to 10^{-9}.

9.1 Isotropic case

First of all, we made some experiments to ensure that the code is able to deal correctly with isotropic materials. We processed several data sets in 2 and 3 dimensions taken from [8] and [12], and got the same results.

For example, in [8], we can find some graphics related to a plane domain consisting of two materials M_1 and M_2. Poisson ratios are $\sigma_1 = 0.17$ and $\sigma_2 = 0.29$. Young modulus are $E_1 = 1$ and $E_2 = 4(1+\sigma_2)E_1/(1+\sigma_1)$. Lamé coefficients are deduced from the formulas

$$\lambda = \frac{E\sigma}{1-\sigma-2\sigma^2} \quad \text{and} \quad \mu = \frac{E}{2+2\sigma}.$$

For a slit-domain, $\omega_0 = 0°$, $\omega_2 = 360°$ and ω_1 runs from ω_0 to ω_2. With Neumann boundary conditions and a step size for ω_1 equal to $1°$, it takes 207 seconds to compute 3444 exponents and obtain the same figure as the one shown in that paper.

9.2 Variation of the opening

We refer here to an example taken from [10]. Two anisotropic materials occupy the upper half plane as shown in Figure 3, graphite between 0 and ω_1, adhesive between ω_1 and π.

Both are orthotropic axisymmetric materials. The coefficients of Hooke's law are for graphite

$$c_{11} = c_{22} = 20.41337, \quad c_{12} = 0.91860168, \quad c_{66} = 1.1, \quad c_{16} = c_{26} = 0,$$

and for adhesive

$$c_{11} = c_{22} = 1.5384615, \quad c_{12} = 0.461538, \quad c_{66} = 0.7, \quad c_{16} = c_{26} = 0.$$

Dirichlet boundary conditions are assumed.

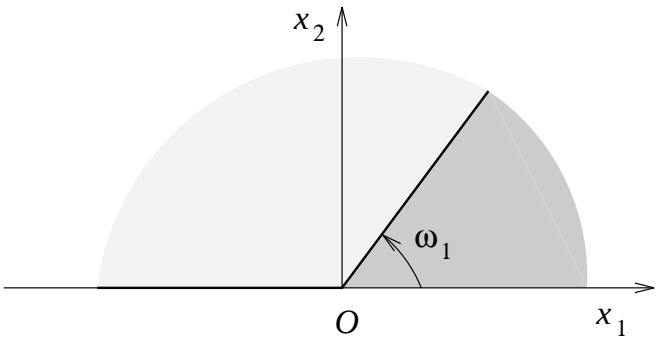

Figure 3

Figure 4 shows the real and imaginary part of the exponents of singularities with respect to the opening angle ω_1, which varies from $0°$ to $180°$ by step of half a degree. Real exponents are represented by dots, complex ones by circles (on reduced graphs, they appear as bold lines). The

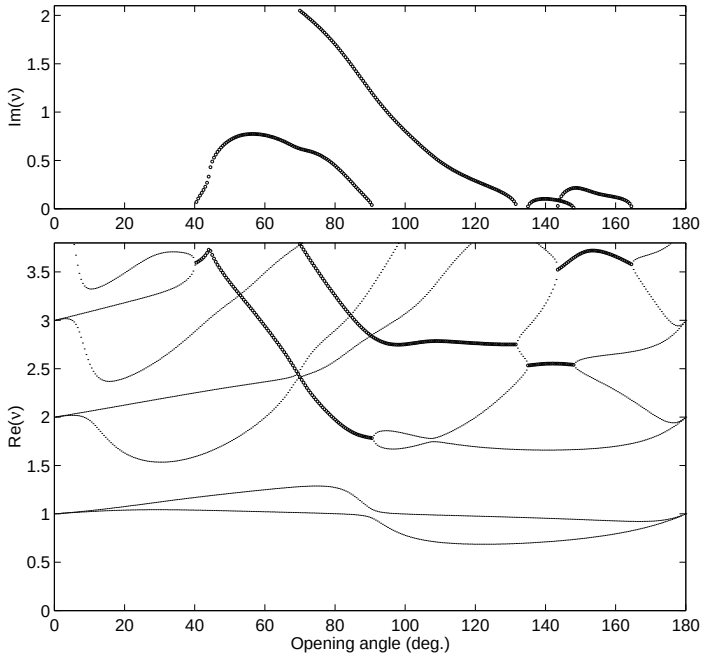

Figure 4

computing time for all these exponents is 148 seconds, including time for some more with real part greater than 3.8. This graph is the same as the one presented in [10].

At the top of the graph, we notice a peak of the curve of the real part near $\omega_1 = 44°$. We made a zoom near this point : beyond the limit of the graph in Figure 4, there exists a quasi symmetric curve, where the imaginary parts are crossing (see Figure 5). By changing the value of the data coefficient c_{11} to 1.33 in the adhesive, we get the Figure 7. Finally, for $c_{11} = 1.41$, we get the Figure 6 which shows a complex crossing point.

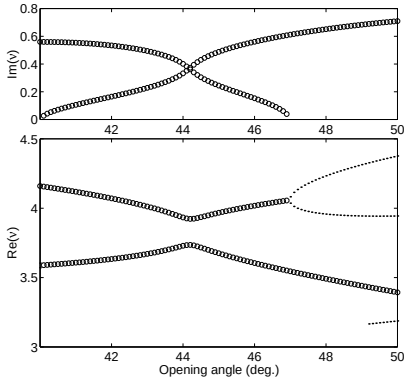

Figure 5

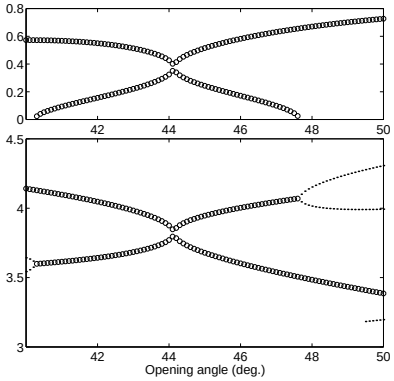

Figure 6

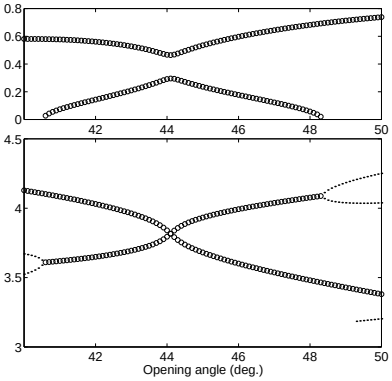

Figure 7

We have a better view of the phenomenon by plotting the exponents in the complex plane, which is shown on the Figures 8, 9 and 10, corresponding to $c_{11} = 1.5384615, 1.41$ and 1.33 respectively (real exponents have been discarded). We can notice that the distance between two points grows while approaching the crossing point. As the values of the opening angle are equidistant, this manifests an important variation at this point. Moreover, if we compute in a smaller region surrounding this point, we get exactly the same kind of graph.

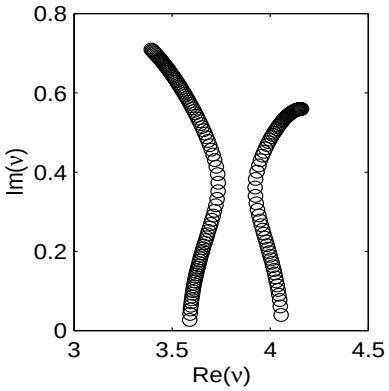

Figure 8

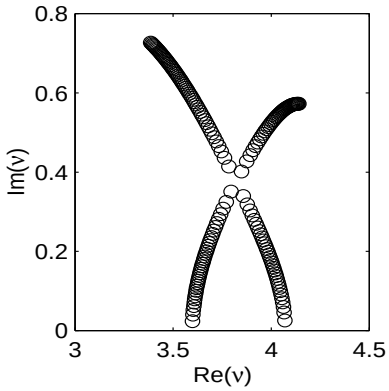

Figure 9

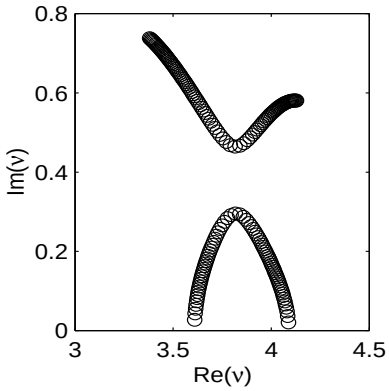

Figure 10

9.3 Multi-material internal interface

We refer here to [12] where we can find five 3D examples with numerical results. We tested these five examples and got exactly the same results, at least up to the significant digits given in the paper.

One of the examples, also treated in [9], is an internal edge lying on $(O, \vec{z})$, intersection of three domains as shown in Figure 11. Each domain is made of the same orthotropic material (fiber/resin composite) with different fiber orientations.

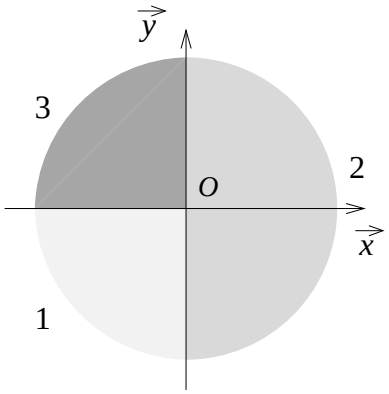

Figure 11

The rigidity matrix is the inverse of the compliance matrix given below :

$$\begin{pmatrix} 1/E_1 & & & & & \\ -\nu_{12}/E_1 & 1/E_2 & & & & \\ -\nu_{13}/E_1 & -\nu_{23}/E_2 & 1/E_3 & & (sym.) & \\ 0 & 0 & 0 & 1/G_{23} & & \\ 0 & 0 & 0 & 0 & 1/G_{13} & \\ 0 & 0 & 0 & 0 & 0 & 1/G_{12} \end{pmatrix}$$

$$E_1 = E_3 = 0.105,\ E_2 = 1,$$

$$G_{12} = G_{13} = G_{23} = 0.0425,$$

$$\nu_{12} = 0.02205,\ \nu_{13} = \nu_{23} = 0.21.$$

With the previous data, the fiber direction is $\vec{y}$ and the rotations θ_1, θ_2 and θ_3 of each material are measured in the $(\vec{y}, \vec{z})$ plane counterclockwise around $\vec{x}$.

In the first test, we have $\theta_1 = -\theta_3 = 45°$ and $\theta_2 = 0°$. The first three exponents found are $\nu_1 = 0.9174569$, $\nu_2 = 0.9812413$ and $\nu_3 = 1$. On Figure 12, the angular singular function is given for ν_1 : it looks quite similar to the result presented in [12]. The exponent $\nu_3 = 1$ has multiplicity 4 and the associated singular functions have no logarithmic terms.

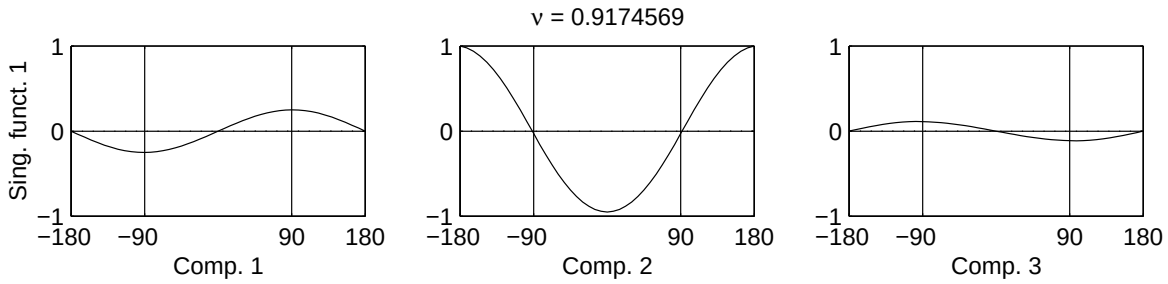

Figure 12

In the second test, θ_2 is varying from 0° to 90° by step of 1°, while $\theta_1 = -\theta_3 = 45°$. The exponents are searched with real part in [0.9,0.99] for each value of θ_2 (1 is still a multiplicity 4 exponent). One can see the result in Figure 13. The curves, computed in 71 seconds, fully corroborate those given in [12].

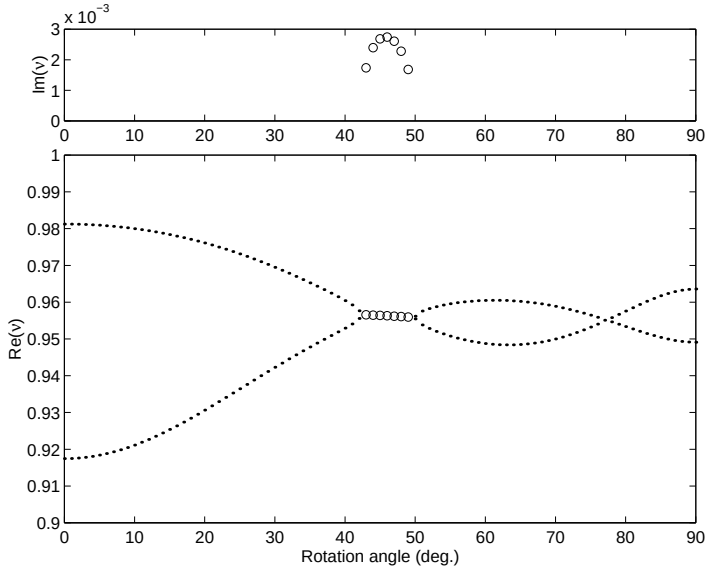

Figure 13

9.4 Internal crack

We consider here an internal crack defined by the half-plane $(O\ ; -\vec{y}, \vec{z})$ as shown in Figure 14.

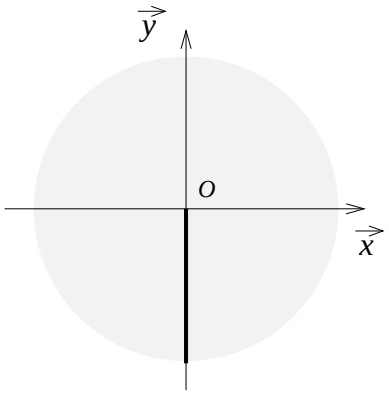

Figure 14

The material is orthotropic and is the same as in § **9.3**. Neumann boundary conditions are assumed. The first exponent $\nu_1 = 0.5$ has multiplicity 3. The associated singular functions have no logarithmic terms. Their angular parts are presented in Figure 15.

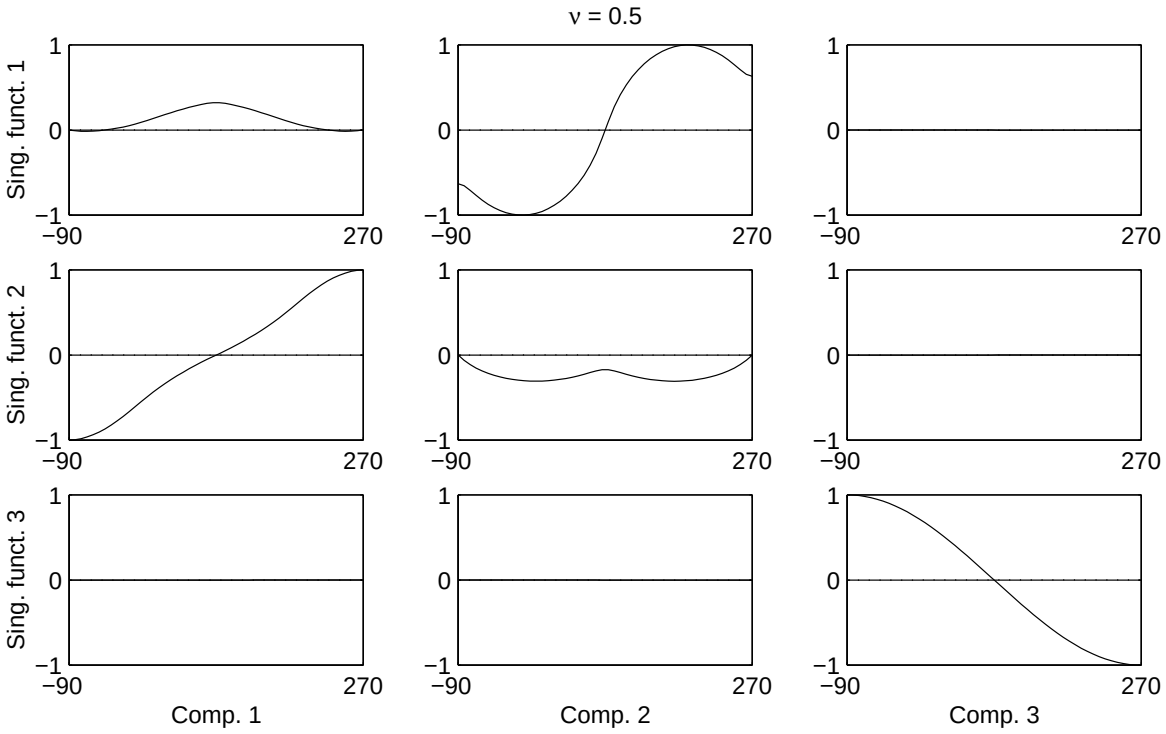

Figure 15

9.5 Edge tracking

To illustrate another kind of computations in three dimensions, we consider the cylindrical object shown in Figure 16, that consists of two parts : a truncated cone (the "cork") made of material M1 and its complementary in the cylinder (the "neck") made of material M2. Boundary conditions are Neumann on the two bases of the cork and Dirichlet on the exterior of the neck. Between the two materials, transmission conditions apply.

The exponents of singularities are computed along the three edges defined by this object and shown in Figure 16. Axes are moved along each edge so that during the rotation around $\vec{x_1}$, the axis of revolution of the object, vector $\vec{x_3}$ is always tangent to the edge.

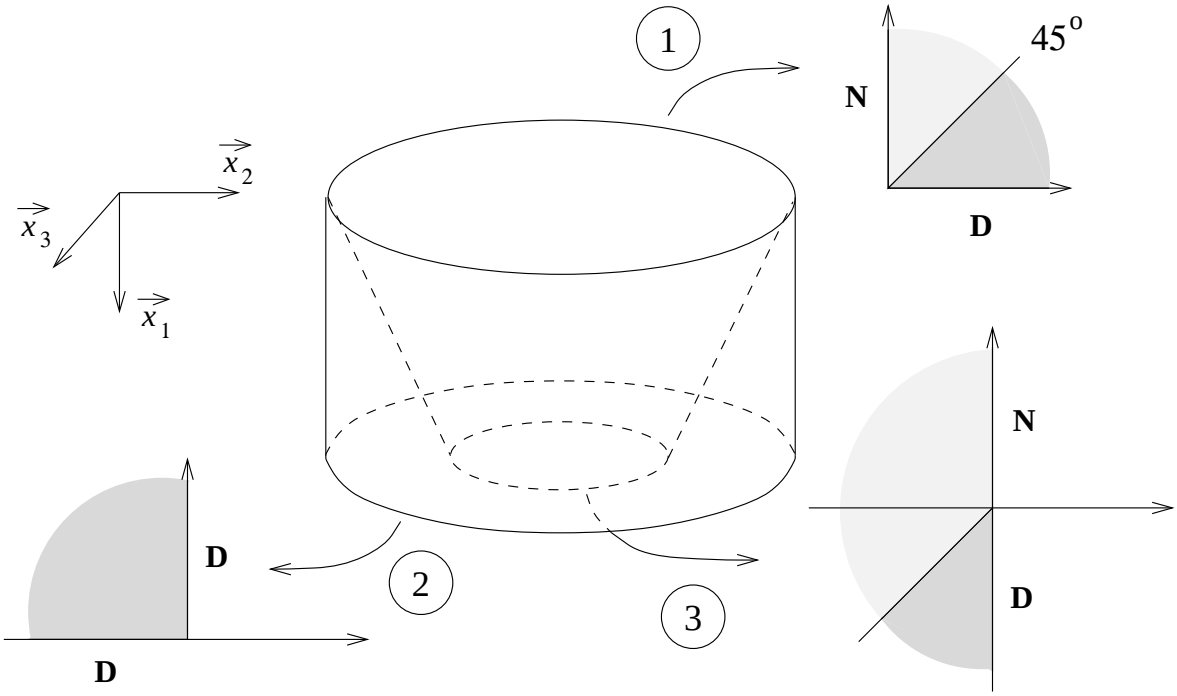

Figure 16

We consider the following two examples.

- Example 1 : Material M1 isotropic, material M2 orthotropic.

  For material M1, Poisson coefficient σ and Young modulus E are set to $\sigma = 0.35$ and $E = 1$.

  With respect to the Lamé coefficients given in § **9.1**, the non-zero coefficients of Hooke's law for material M1 are then

$$c_{11} = c_{22} = c_{33} = \lambda + 2\mu, \quad c_{44} = c_{55} = c_{66} = \mu, \quad c_{12} = c_{13} = c_{23} = \lambda.$$

  For material M2, the non zero coefficients of Hooke's law are

$$c_{11} = 1.27,\ c_{22} = 2.27,\ c_{33} = 14.5, \quad c_{44} = c_{55} = 0.485, \quad c_{66} = 0.324,$$
$$c_{12} = 0.622,\ c_{13} = c_{23} = 0.672.$$

Results are given in Figures 17, 19 and 21 respectively corresponding to edges 1, 2 and 3, with computing times 93 seconds, 32 seconds and 265 seconds.

- Example 2 : Material M1 orthotropic, material M2 anisotropic without any particular structure.

Material M1 is material M2 of example 1. For material M2, the non zero coefficients of the Hooke's law are

$$c_{11} = 2.27,\ c_{22} = 16.27,\ c_{33} = 10.5, \quad c_{44} = c_{55} = 0.485, \quad c_{66} = 0.324,$$
$$c_{12} = 0.522,\ c_{13} = 0.672,\ c_{23} = 0.272,\ c_{25} = -0.3,\ c_{35} = 1.0,\ c_{26} = 0.1,\ c_{46} = -0.1\,.$$

Results are given in Figures 18, 20 and 22 respectively corresponding to edges 1, 2 and 3, with computing times 140 seconds, 33 seconds and 282 seconds.

We can make the following remarks :

. every graph is 2π-periodic as expected,

. moreover, in example 1, the variation of the exponents is π-periodic due to the nature of the materials involved, unlike in example 2 where we can see the influence of material M2.

On Figures 18 and 22, rotation angle varies from $-20°$ to $340°$ to better see what happens near angle $0°$.

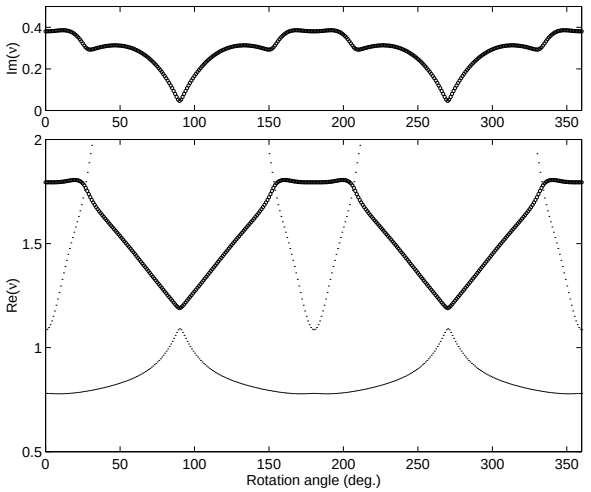

Figure 17

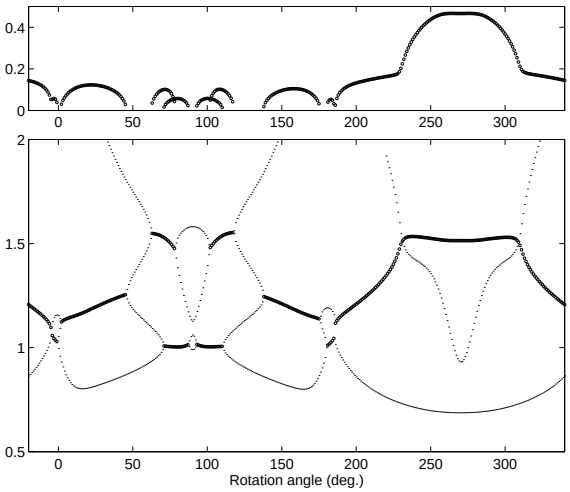

Figure 18

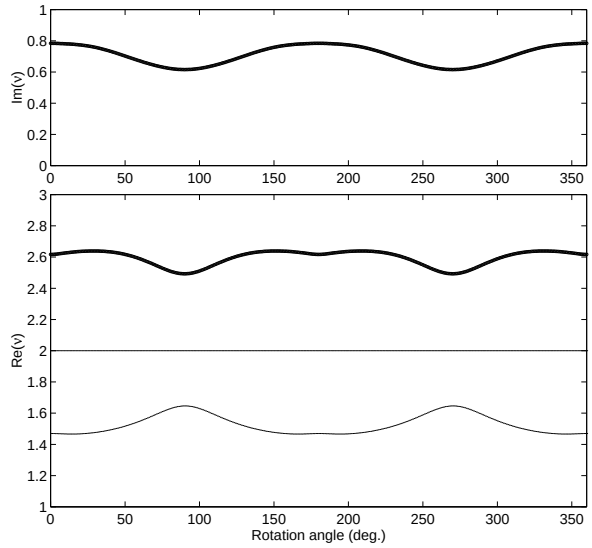

Figure 19

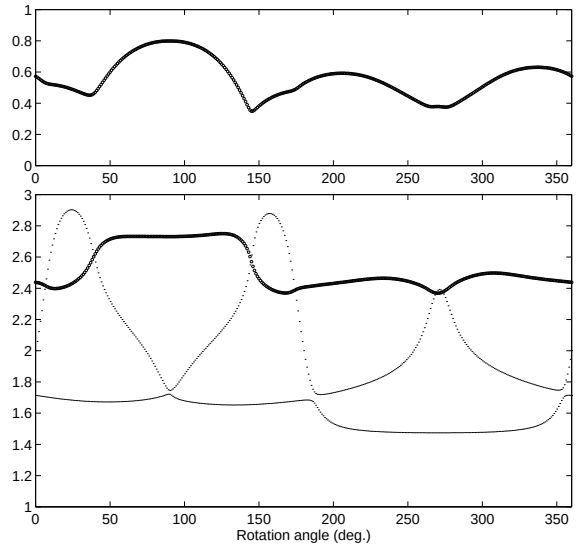

Figure 20

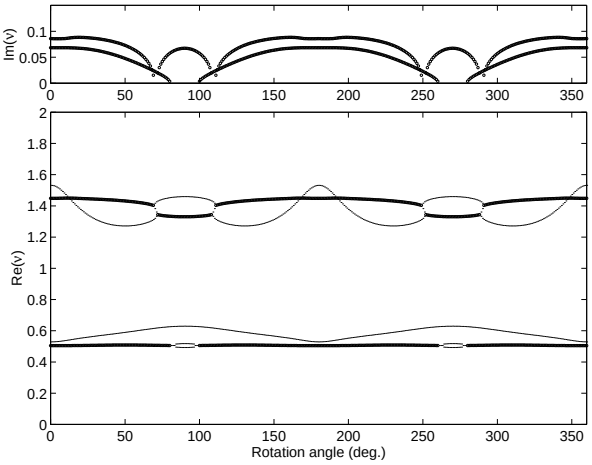

Figure 21

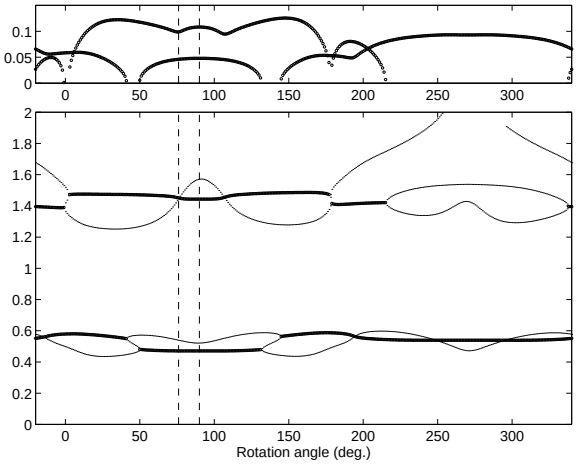

Figure 22

We now illustrate the computation of singular functions, by considering the edge 3 of the second example, with rotation angles 76° and 90°. The first exponents shown by the dashed lines in Figure 22 are :

. for 76° : $\nu_1 = 0.471024 + 0.046111i, \nu_2 = 0.538880, \nu_3 = 1.447458, \nu_4 = 1.450971 + 0.098823i$,

. for 90° : $\nu_1 = 0.471017 + 0.048029i, \nu_2 = 0.521243, \nu_3 = 1.443551 + 0.108177i, \nu_4 = 1.571289$.

The angular singular functions are given in Figure 23 for 76° and in Figure 24 for 90°. We can make the following remarks :

. the general shape of the angular singular functions has more variations as the modulus of the exponents grows,

. at the frontier of the two domains, the angular singular functions are continuous but not differentiable.

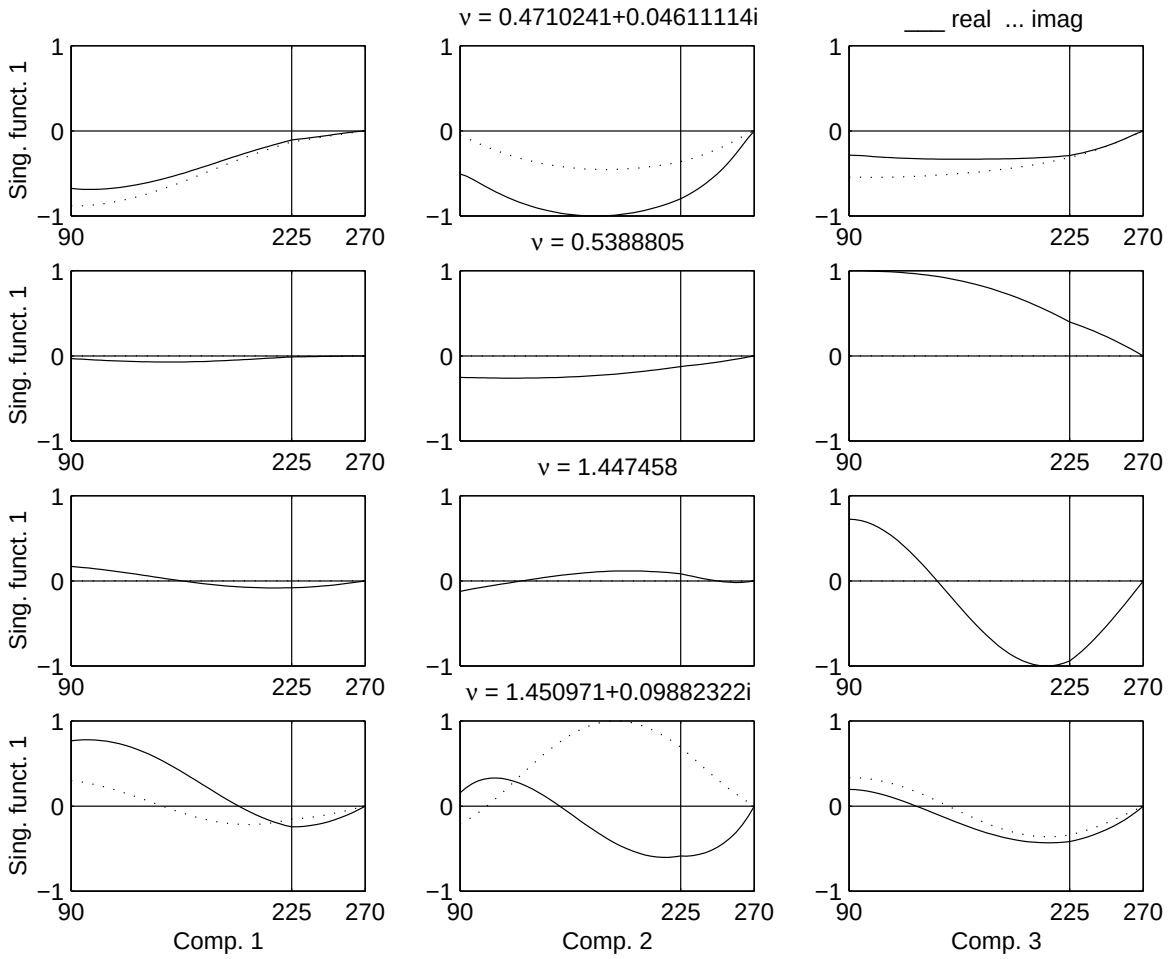

Figure 23

This test is also interesting because it is a good indication of the correctness of the method. Looking at the Figure 24 for the angle 90°, one can notice that the angular singular functions associated with ν_1 and ν_3 have zero third components, while the angular singular functions of ν_2 and ν_4 have zero first two components. This characteristic behaviour is well known when the materials are isotropic, which is not the case here. However, introducing the coefficients computed for this angle in the equations, leads to a system where the third component is uncoupled from the first two. This explains this behaviour, which is due to the properties of the particular materials involved.

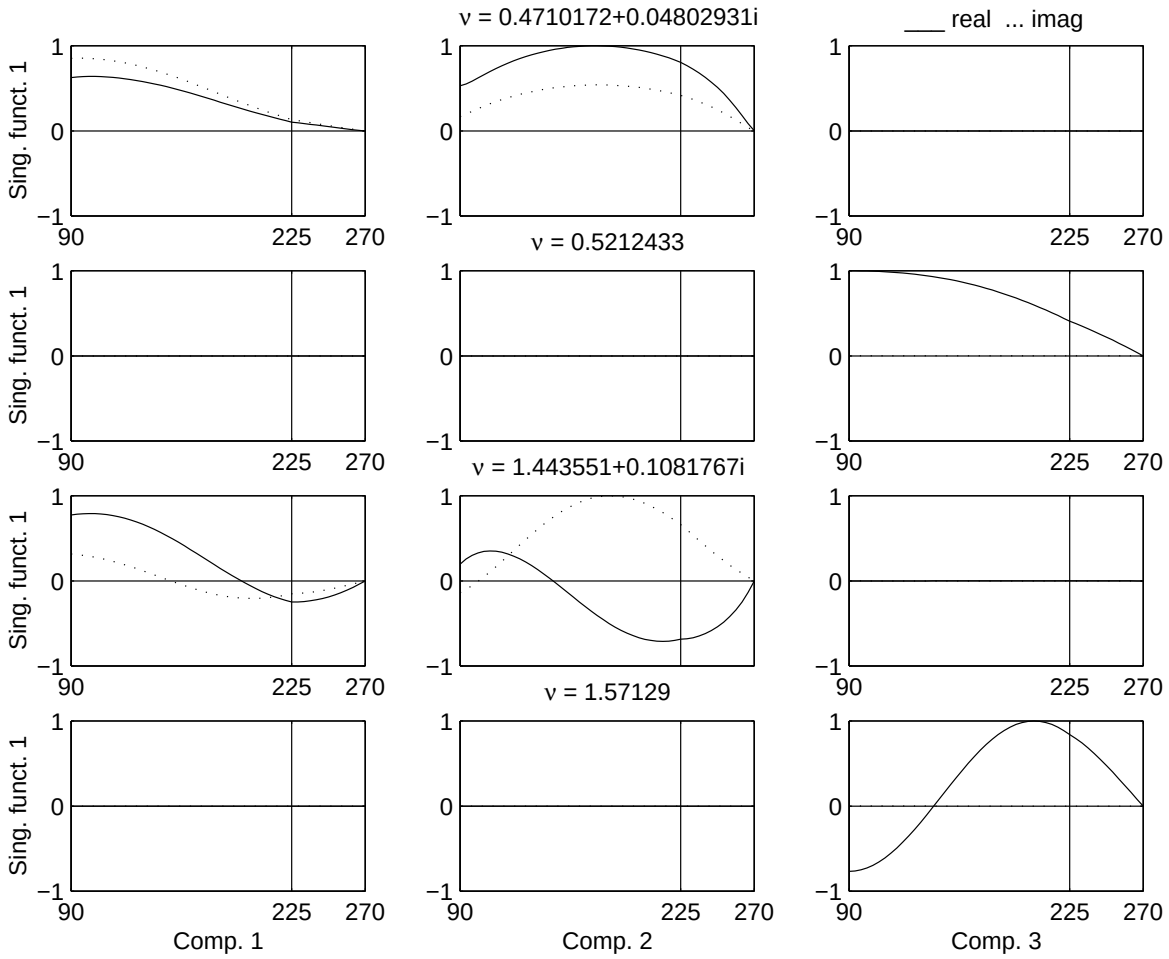

Figure 24

The object considered in this section is rather simple in that the rotation is made around an axis, $\vec{x_1}$, which is one of the absolute axes. More complicated situations can be considered easily, provided we can obtain, in each point of calculation :

. the orientation of the local axes with respect to the absolute axes, given for instance by a rotation matrix,

. the geometry of the domain (opening of the angular sectors Γ_k).

As an example, we suppose that the previous object is cut by the plane $x_1 = -\tan\alpha\ x_2$, as shown in Figure 25.

With $\alpha = 30°$, along the edge 2, which is now an ellipsis, the geometry of the domain is varying from 60° to 120°. The computation time is 40 seconds and the results are given in Figure 26.

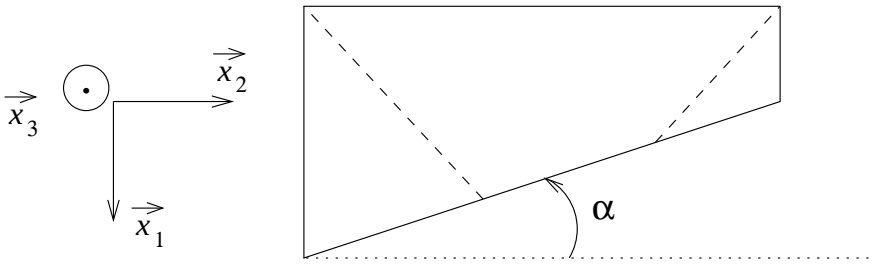

Figure 25

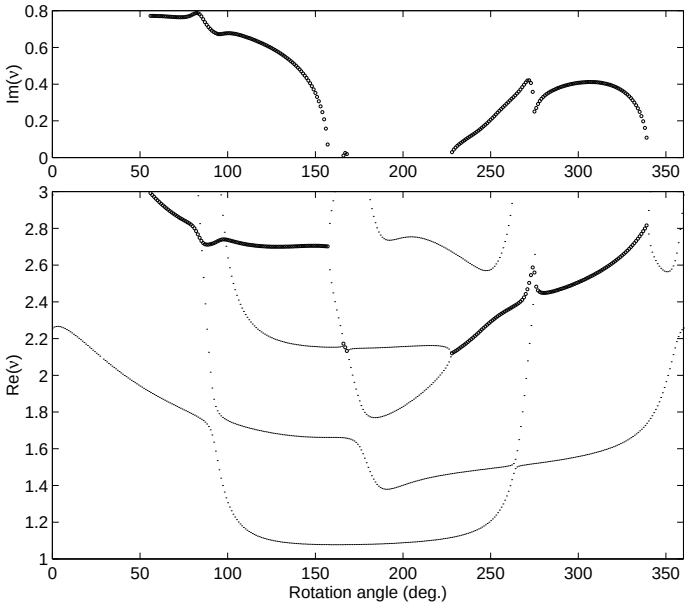

Figure 26

10. Conclusion

In this paper, we have presented a method for the computation of singularity exponents in linear elasticity, which is especially useful in the anisotropic case. The method is based on the construction of a matrix of low dimension depending on a complex variable ν, whose determinant is zero for a discrete set of values of this variable. These values are the exponents of singularities.

Except during the preliminary step which consists of the computation of the roots of a certain polynomial associated with the system, the construction of this matrix is analytic. As a consequence, we get a method which is reliable, rapid and easy to use as the various examples given show.

In all situations when the singular functions are homogeneous functions $r^\nu g(\theta)$, we are able to compute their angular part g and our method proves to be efficient even if there is multiplicity. In the isotropic case, our results have been successfully compared with those deduced from analytic formulas given in [4], using only the exponent ν. The exceptional cases where logarithmic terms appear in the singular functions can be detected with our method. The analytic expressions for

the singular functions in this case differ, however, from the generic case, and are available from [1], but they are not implemented here.

Finally, due to its data structure, our program is particularly adapted to the study of parameter dependency and moreover can be coupled with other codes. The geometrical and material input data could be provided by another code, while the output (exponents and angular functions) can be post-processed in view of further investigations.

References

[1] M. Costabel, M. Dauge. Construction of corner singularities for Agmon-Douglis-Nirenberg elliptic systems. *Math. Nachr.* **162** (1993) 209–237.

[2] M. Costabel, M. Dauge. Computation of corner singularities in linear elasticity. *Lect. Notes Pure and Appl. Maths* **Vol. 167** (1994) 59–68.

[3] M. Dauge. *Elliptic Boundary Value Problems in Corner Domains – Smoothness and Asymptotics of Solutions*. Lecture Notes in Mathematics, **Vol. 1341**. Springer-Verlag, Berlin (1988).

[4] P. Grisvard. Singularities in boundary value problems, RMA 22, Masson, France (1992).

[5] V. A. Kondrat'ev. Boundary-value problems for elliptic equations in domains with conical or angular points. *Trans. Moscow Math. Soc.* **16** (1967) 227–313.

[6] D. Leguillon, E. Sanchez-Palencia. Computation of singular solutions in elliptic problems and elasticity. John Wiley & Sons, New York, N Y, (1987).

[7] S. Nicaise. *Polygonal interface problems*. Methoden und Verfahren der Mathematischen Physik, **39**. Verlag Peter D. Lang, Frankfurt-am-Main (1993).

[8] S. Nicaise, A.-M. Sändig. General interface problems I. *Math. Meth. Appl. Sci.* **17** (1994) 395–429.

[9] S. S. Pageau, S. B. Biggers Jr. A finite element approach to three-dimensional singular stress states in anisotropic multi-material wedges and junctions. *Int. J. Solids Structures* **33** (1996) 33–47.

[10] P. J. Papadakis, I. Babuška. A numerical procedure for the determination of certain quantities related to the stress intensity factors in two-dimensional elasticity. *Comput. Methods Appl. Mech. Engrg.* **122** (1995) 69–92.

[11] Z. Yosibash., B. Szabo. Numerical analysis of singularities in two-dimensions, Part 1 : Computation of eigenpairs. *Int. J. Num. Meth. Eng.* **38** (1995) 2055–2082.

[12] Z. Yosibash. Computing edge singularities in elastic anisotropic three-dimensional domains. *Int. J. Fracture* **86** (1997) 221–245.